The Brazilian Electric Propulsion Program

IEPC-2007-147

Presented at the 30th International Electric Propulsion Conference, Florence, Italy
September 17-20, 2007

Gilberto M. Sandonato[1], José Américo N. Gonçalves[2], Ricardo T. Irita[3], George F. Fernandes[4], Paolo Gessini[5],

Instituto Nacional de Pesquisas Espaciais, São José dos Campos, SP, 12227-010, Brazil

And

Rodrigo I. Marques[6], and Stephen B. Gabriel[7]

University of Southampton, Southampton, United Kingdom, SO17 1BJ

Abstract: This paper presents a review of the Brazilian electric propulsion programs related to the development both of Kaufman-type ion thrusters and Pulsed Plasma Thrusters at the National Institute for Space Research (INPE), and the Hall thrusters at the University of Brasilia (UnB). The past and present development status and the trends of the Brazilian electric thrusters are presented and discussed as well.

Nomenclature

T	=	thrust
I_s	=	specific impulse
I_b	=	beam current
I_K	=	keeper current
I_D	=	discharge current
m	=	propellant mass
$\dot{m}_j$	=	propellant mass flow rate,*(j: M main discharge, H main cathode and N neutralizer)*
U	=	accelerating voltage
U_D	=	discharge voltage
q	=	ion charge
g_o	=	9,81 m/s^2

I. Introduction

ELECTRIC thrusters have been developed in the last 23 years by the Associated Plasma Laboratory (LAP), at the National Institute for Space Research (INPE), aiming new propulsive technologies for the satellites of the Brazilian Complete Space Mission (MECB). Since the 80's decade, LAP has concentrated its efforts on Kaufman-type ion thrusters, which could produce thrust levels in the range of 1 to 10 mN for

[1] Senior Researcher, Associated Plasma Laboratory, gms@plasma.inpe.br
[2] Senior Researcher, Associated Plasma Laboratory, americo@plasma.inpe.br
[3] Senior Researcher, Associated Plasma Laboratory, irita@plasma.inpe.br
[4] Graduate Student, Associated Plasma Laboratory, georgeff@plasma.inpe.br
[5] Postdoctoral Research Fellow, Associated Plasma Laboratory, paolo@plasma.inpe.br
[6] PhD candidate, Astronautics Research Group, intini@soton.ac.uk, Researcher, at INPE-LCP
[7] Professor, Astronaut Research Group, sbg2@soton.ac.uk

station-keeping. This program produced prototypes with different sizes, besides the spin-off technologies related to hollow cathodes and other components. Nevertheless, the Brazilian interest on electric thrusters does not reside only in Kaufman-type ion thruster but also in Pulsed Plasma Thrusters (PPT) and Hall Thrusters, presently under development at the Associated Laboratory of Combustion and Propulsion at INPE and at the University of Brasilia (UnB), respectively.

Although the amount of money invested in these programs does not exceed few hundreds thousands of dollars per year, besides the small staff engaged on them, both the financial and technological barriers have been overcome thanks to dedication and creativity of all the researchers. Therefore, more than a report of the Brazilian activities on electric propulsion, this paper presents the practical alternatives adopted by the Brazilian researchers to overcome all challenges.

II. Evolution of the Brazilian Ion Thrusters

A. Electric propulsion at INPE

The National Institute for Space Research (INPE) is one among the various institutes of the Ministry of Science and Technology (MCT) of the Brazilian Federal Government. In the past four decades, INPE has been dedicated to a wide range of space activities involving various laboratories, in particular the Associated Plasma Laboratory (LAP), which was established in 1978, becoming the first associated laboratory of INPE in 1986. During the past two decades LAP has been recognized by the quality of various experiments and activities carried out in such diverse areas as: simulation in the laboratory of space plasma phenomena; isotopic enrichment; surface processing of materials; fusion plasma research, including the development of a spherical torus for advanced magnetic confinement studies and microwave devices for plasma heating experiments, the implementation of plasma diagnostic techniques; and development of plasma technologies for electric propulsion as well.

In 1985 the laboratory started the PION (ion propulsion program) and in 2004 the PROPEL (electric propulsion program) was formally supported by the Brazilian Space Agency (AEB), both ones dedicated to the study of electrostatic propulsion and the development of Kaufman-type ion thrusters for auxiliary propulsion of satellites. These two programs have produced a series of four prototypes involving models of 5-cm (two models), 7-cm and 15-cm diameters ion thrusters.

- **The Associated Plasma Laboratory (LAP)**

1. Past and Present Ion Thrusters

The first demonstration prototype of ion thruster (PION-1), built in 1985, consisted of a 7-cm diameter by 14-cm long stainless steel discharge chamber, a checkerboard magnetic assembly produced by ferrite permanent magnets, a pair of 30% transparency stainless steel grids masked down to a 3 cm exhausting section, and tungsten filaments as primary electron emitters for both the main discharge and neutralizer. This ion thruster and its narrow argon beam are both shown in Fig.1a and 1b. The performance tests were carried out in the first vacuum chamber using argon as propellant, the flow of which was set by needle valves (since there were no flow meters available at that time). The experiments comprised only the measurement of both the plasma density in the discharge chamber, using Langmuir probes, and the ion beam current, using a Faraday cup. Because of the poor overall performance a maximum thrust of 2.7 μN was estimated for an accelerating voltage of 900 V (see Table 1) even generating plasma densities of order of 10^{16} m^{-3}. The thrust was estimated using the well known thrust to beam current relationship, assuming a single charged ion beam (see Eq.1 in the Appendix).

The second enhanced prototype (PION-2) was built in 1992. This model was designed using self consistent analytical methods,[1-3] for both the ion optics system and the discharge chamber. It consisted of a 5-cm diameter by 10-cm long stainless steel discharge chamber, a ring cusp magnet assembly produced by SmCo permanent magnets, one coaxial oxide cathode (thermionic emitter), a pair of 45% transparency tantalum grids masked down to 4cm exhausting section, and a surrounding mu-metal magnetic shield. The PION-2, shown in Fig. 2a, was tested inside the larger vacuum chamber using argon as propellant and the diagnostics were the same ones as those used for PION-1. The differences in the performances between these two models were remarkable (compare the ion beams in Fig. 1b and Fig. 2b). For a same level of plasma density generated in both prototypes, PION-2 produced higher argon ion beam currents (typically 20 mA) which result in an estimated thrust level of 559 μN and an estimated specific impulse of 191 s (see Eq. 2 in the Appendix), at an accelerating voltage of 1000 V and a mass flow rate of 298 μg/s, as listed in Table 1. The

low value obtained for the specific impulse comes from propellant leaks through the PION-2 joints, which were not properly sealed by any welding techniques but only assembled by fastening them with screws.

Another limiting factor for a better efficiency of this prototype was the short lifetime of the oxide cathodes (no more than few hundreds of hours), because the materials used were not resistant enough to the ion bombardment. The cathode were usually damaged either by losing its oxide layer for low discharge currents, or, by melting its nickel basis for discharge currents exceeding 1 A.

The third and present ion thruster prototype (PION-3) was designed by Particle in Cell numerical codes (PIC), aiming both an enhanced plasma generation and an efficient ion beam extraction. It consists of a 16-cm diameter by 5-cm long stainless steel discharge chamber, a ring cusp magnet assembly produced by a pair of AlNiCo ring permanent magnets, a pair of 50% transparency molybdenum grids, and a surrounding mu-metal magnetic shield. A rolled-tantalum-oxide-foil-insert hollow cathode has been used for the main discharge and a dispenser insert hollow cathode has been used as neutralizer. The late being a commercial type one. The PION-3, shown in Fig. 3a and its argon ion beam in Fig. 3b, is presently under the ground-based tests in the larger vacuum chamber. Its preliminary performance parameters and results are both listed in Table 1. These results are the preliminary ones, since the complete performance characterization will involve a more careful exploration of the PION-3 capabilities, besides an accurate thrust measurement using the pendulum target balance presently under development at LAP. Nevertheless, the estimated thrust of 4 mN, with a specific impulse of 1183 s, at 500 V accelerating voltage, indicates that this prototype exhibits real possibilities to achieve higher thrust levels once some improvements were adopted, e.g., the elimination of propellant leaks.

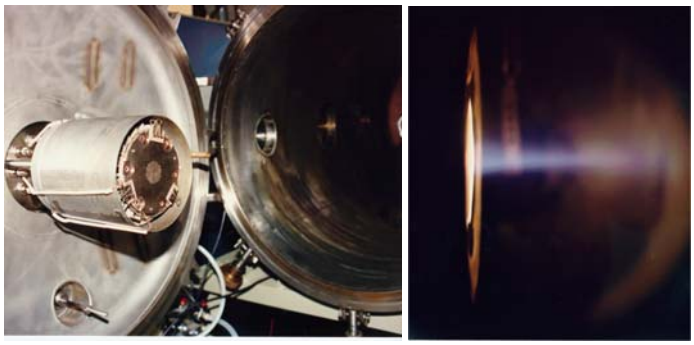

a) b)

Figure 1. 7-cm ion thruster, PION-1 (a), and firing (b).

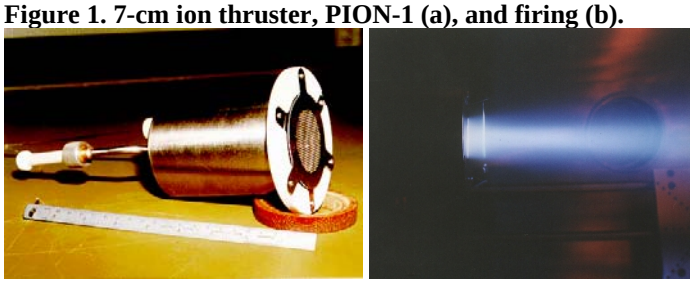

a) b)

Figure 2. 5-cm-exhausting ion thruster, PION-2 (a), and firing (b).

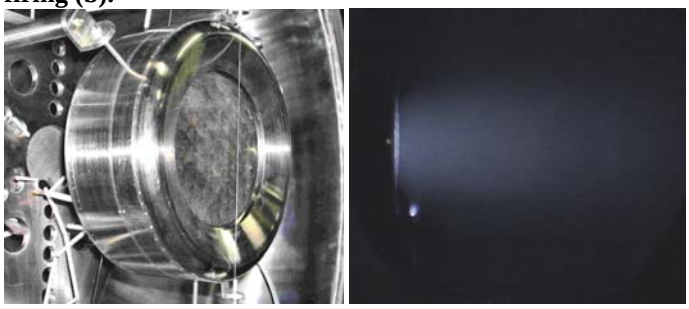

a) b)

Figure 3. 16-cm ion thruster, PION-3 (a), and firing (b).

Table 1. Kaufman-type Ion Thrusters Performance Parameters and Results. Propellant: argon

Model	**Main Discharge**				**Ion Beam**		**Neutralizer**			**Calculated values**	
	U_D	I_D	$\dot{m}_M$	$\dot{m}_M$	U	I_B	U_K	I_K	$\dot{m}_N$	T Eq. 1*	I_s Eq. 2*
PION-I	50	1			900	17				0.45	
PION-2	100	0.6	298		1000	20	30	0.2		0.56	191
PION-3	40	8	160	96	500	200	150	2	96	4	1183
	V	A	µg/s	µg/s	V	mA	V	A	µg/s	mN	s

*See Appendix

The fourth ion thruster prototype (PION-4), shown schematically in Fig.4a, is currently under assembling. It consists of a 6-cm diameter by 16-cm long stainless steel discharge chamber, a pair of 50% transparency tantalum grids masked down to a 5 cm exhausting section. The artistic conception of the discharge chamber

assembled with the grids is shown in Fig. 4b. A rolled-tantalum-oxide-foil-insert hollow cathode will be used for the main discharge and a dispenser hollow cathode will be used as neutralizer. Its magnetic assembly consists of a solenoid and an AlNiCo ring permanent magnet radially magnetized. This setup will allow a more flexible and precise adjustment of the magnetic containment volume of electrons, since the magnetic field strength will be dictated by the solenoid current. A mu-metal magnetic shield surrounds the discharge chamber, as shown in Fig. 4c. The PION-4 is planned to be under the ground-based performance tests in the next year of 2008.

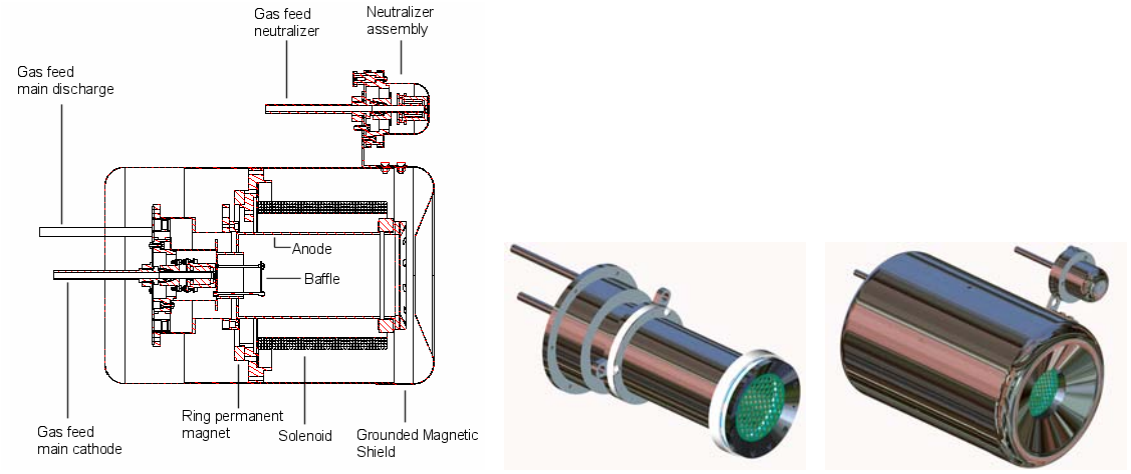

a) b) c)

Figure 4. Schematic diagram of the 5-cm ion thruster (PION-4) (a), and both artistic conceptions of the discharge chamber with the grids (b) and the external magnetic shield (c).

2. Components

As mentioned above, the LAP ion thrusters started running with tungsten filaments, which were replaced by oxide cathodes, and presently they are equipped with rolled-tantalum-oxide-foil hollow cathodes. All these cathodes were entirely developed and built at LAP.

The present hollow cathode consists of a 5-mm diameter by 40-mm long, 0.3-mm-wall thickness tantalum tube, with a cold-pressed 1-mm diameter orifice tungsten tip. The insert consists of a 5-turns rolled tantalum foil painted with a thin layer of mixed carbonates, (Ca, Ba, Sr)CO_3, which are converted to oxides by heating the insert up to 900 ^{o}C. The cathode heater comprises a boron nitride body machined in the shape of a revolver cylinder, in which holes a coiled tungsten filament is passed through, as shown in Fig. 5a. This heater expends 90 W to heat the cathode up the carbonate to oxide conversion temperature. As there are no commercial standard pipe fittings for 5 mm-diameter tubes, both the connector and the ferrules must be developed and machined specially for sealing the cathode body. The present hollow cathode full assembly is shown in Fig.5b. The preliminary experimental tests have revealed that this hollow cathode can operate at currents in the range of 3 to 10 A for long time periods, and at 18 A for short time periods. This cathode is still under investigation aiming both at its complete performance characterization and performance enhancement.

a) b)

Figure 5. Rolled-tantalum-oxide-foil hollow cathode: heater cartridge (a) and fully assembled (b).

3. The pendulum target thrust balance

The various methods for the measurement of thrust fall into two general categories. Direct methods, where the thruster is suspended on a thrust balance, the displacement of which is measured by a sensor, and indirect methods, where the thruster is fixed and the displacement of a target balance, which is impacted by the thruster exhaust, is measured. These latter techniques present several advantages over direct methods. The sensitivity of the balance is inversely proportional to the weight of the moving part and, if the thruster is

mounted on it, this may be quite heavy. In addition to limiting the instrument sensitivity, this also causes frictional losses due to the suspension. Unless the whole propulsion system is mounted on the balance, as could be the case with an Ablative Pulsed Plasma Thruster (APPT), [4,5] electric power cables, propellant feed lines and, possibly, cooling flow lines will cause a high motion resistance.[6,7] Target systems are currently being used by other investigators for the measurement of momentum and heat fluxes in plasma environments.[8] The thrust balance designed to perform measurements at INPE is, essentially, a physical pendulum, mounted on knife-edge suspensions.

In order to decrease the uncertainty in the measurements due to the imperfectly known plume momentum transfer modalities, the design of the actual target is based on the "cylindrical target" developed by Yanagi and Kimura at the University of Tokyo[9,10] and successfully employed by Japanese investigators. The target consists of a series of discs connected to a back plate, as shown in Fig. 5. The front disc presents a hole much smaller than the successive ones. The device is positioned in such a way that the thruster plume enters through the front hole, with negligible impingement on the outer surface. Depending on the plume divergence, some of the particles may or may not hit the other discs, but the majority will impinge on the back plate, which has a conical shape to maximize dispersion. As the opening area normal to the radial direction is much larger than that normal to the axial direction the particles, rebounding with different trajectories, will hit the discs and, after various collisions, escape with an essentially radial momentum.

This target design realizes a nearly total transfer of the plume axial momentum to the target, without any assumption about the exact modalities of particle-surface interaction. It therefore allows a measurement of the thrust closely approximating that obtainable with a direct method, but with a much simpler device. A comparison between Ablative Pulsed Plasma Thruster (APPT) thrust measurements obtained with the plume impinging on the Japanese cylindrical target and with the thruster mounted on a torsion-type thrust stand shows that the former method, as expected, gives results consistently higher than the latter,[11] but only by 10%, showing that the axial momentum of the rebounding particles is actually minimized.

The development of the thrust balance was planned to be carried out in two phases: the first one comprising the study of the thrust measurement using a calibration prototype in the atmosphere environment, and the second one by building the final model and installing it in the vacuum chamber for following in-situ thrust measurements of ion thrusters. The calibration prototype, which is in the final stage of characterization, consists of a series of 7 galvanized steel AISI 1020 rings (seizing 50-cm external diameter, 40-cm internal diameter and 0.5-mm thickness), galvanized steel AISI 1020 rings centre plate which supports the setup as whole, and a stainless steel AISI 304 target, as shown schematically in Fig. 6a and assembled in Fig. 6b. This prototype weights 10 kg and has a sensibility in the range of 1 to 20 mN with resolution of 1μN, using a laser optical lever of about 2-m optical path. The final model of the thrust balance is under construction and all of its materials were substituted aiming to decrease its weight and to adequate it to better withstands ion

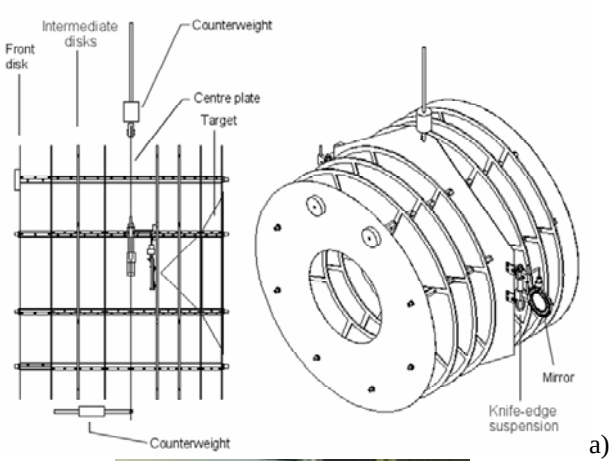

a)

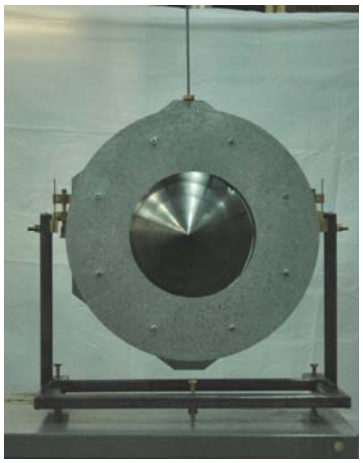
b)

Figure 5. Pendulum target thrust balance schematics (a) and assembled on its support (b)

bombardment. This latter will have the same dimensions as the calibration model and it will be built using aluminum alloy 2024 for the intermediate disks, TiAl6V4 for both the front disk and centre plate, and graphite R7510 for the target. Both models of balance share the same equipment used for the optical laser lever (a HeNe laser, 843nm and 0.8 mW), and for the sensor and data acquisition board (Hamamatsu: S1881 position sensitive detector and C9069 signal processing circuit, respectively).

- **The Propulsion and Combustion Laboratory (LCP)**

4. Past and Present PPT thrusters

In 2002 at the INPE/LCP – Combustion and Propulsion Laboratory – a research was initiated to study pulsed plasma thrusters. This research was carried out as part of a student M.Sc. degree,[12] supervised by Fernando de Souza Costa (INPE/LCP). In 2003 three thrusters were designed, built and tested. These PPTs had a coaxial geometry, copper electrodes and the propellant was Teflon®(PTFE). Fig. 6a shows a diagram of a PPT in a coaxial geometry. In the prototypes tested, a 4.7 mF capacitor was charged with 73 V and discharged at the primary of an auto-transformer (1:150), generating a pulse of approximately 10 kV in the secondary of the auto-transformer, which was then applied onto the propellant surface. In order to verify the effects of the input energy per unit of PTFE exposed area on the propellant mass variation, three discharge chambers were tested, with different exposed propellant areas between the electrodes. Fig. 6b shows a schematic of the discharge chambers.

Table 2 summarizes the test parameters and shows the results of the tests. It was verified that an increase in energy input per propellant area increases the mass consumption per energy unity, when keeping the same energy applied. This was an expected result, in agreement with previous results found in other laboratories.[4] Fig. 7 shows the actual discharge chambers before and after the tests.

In 2004 a new research was initiated, this time as part of a PhD thesis of a student at the University of Southampton in cooperation with INPE/LCP.[13] This research was aimed at increasing the PPT propellant efficiency by applying additional discharge(s) on the surface of the propellant, after the main discharge. In order to minimize the LTA problem a new PPT design was conceived. The approach to solve this problem was to try to electromagnetically accelerate the LTA by employing an additional pulse (or pulses) after the main discharge occurs. However, if these additional pulses were to occur in the same set of electrodes, near the propellant surface, the propellant would receive more heat which would lead to more LTA. Therefore, the additional discharges should take place downstream, relatively far from the surface, in a separate set of electrodes. It was clear also that a synchronization system had to be used to allow the secondary pulses to occur only after the main discharge occurred. Also, it was desirable to have a switch system capable of triggering several pulses in the extra pair of electrodes in order to investigate the effects of the timing and different pulse patterns in the performance of the HFB-PPT. Fig. 8 shows the HFB-PPT discharge chamber.

A HFB-PPT prototype was designed and built at INPE/LCP and tested at the University of Southampton. Fig. 9a shows the computer model of our developed prototype of HFB-PPT with its interface, allowing the thruster to be mounted horizontally or vertically, depending on the type of diagnostics desired. In this prototype the second set of electrodes also acts as divergent nozzle. For diagnostic reasons the prototype was assembled with glass on both sides. A spark plug is also present, close to the first set of electrodes.

Preliminary tests with this prototype were carried out to characterize the thruster. It was used a 110 μF capacitor for the main discharge and a 4700μF capacitor for the secondary discharge. Fig. 9b shows a picture of the HFB-PPT firing. This picture is an integral of the primary and secondary discharges and was taken with 1.5 kV main discharge, 200 V secondary discharge. The high capacitance of the secondary discharge was chosen to investigate maximum lengths of secondary discharges. In this phase the HFB-PPT was tested with three different main discharge voltages (1 kV, 1.5 kV and 2 kV) and fourteen different secondary discharge voltages (0, 3.75, 7.5, 15, 30 35, 50, 75, 100, 150, 200, 250, and 300 V). A single second pulse was employed in all cases and there was no added delay between the first pulse and the second pulse. The intention with these tests was to observe how the currents and voltages of the secondary discharge behave with single pulse and *zero* delay, to serve as a base for future tests. The low voltages applied to the secondary discharges were used to investigate the time of flight and effects of the first discharge on the secondary discharge.

In this mode the HFB-PPT operates like a two-stage solid pulsed plasma thruster. Four distinct regimens were observed during the tests. The regimens are delimited by increasing the second discharge voltage. The first regimen of the secondary discharge is largely dependent on the main discharge that, in fact, generates current between the secondary electrodes even when its capacitor is completely discharged.

The second regimen shows an oscillatory discharge with an offset, given by the increased voltage in the secondary discharge. A critically dumped discharge is observed after the end of the main discharge, although not very pronounced. The third regimen shows a more pronounced critically dumped phase after the main discharge ended and the fourth regimen shows an even more pronounced critically dumped behaviour.

Measurements of the second discharge to investigate its length, delay with respect to the first discharge, and maximum current were carried out. Fig. 10a shows the length of the discharges for all the fourteen voltages of the second discharge at three different main discharge voltages. It can be seen an abrupt change in the length of the discharge at around 75 V and a tendency of an increasing length. For comparison, the main discharge (or primary discharge) length is also plotted.

Fig. 10b shows the measured delays between the first and second discharge. There is a maximum delay observed at different points, depending on the main discharge voltage. For 1 kV main discharge there is a maximum delay at 150 V second discharge. For a 1.5 kV main discharge, the maximum delay is at 200 V and for 2 kV main discharge, the maximum delay occurs at 250 V.

The maximum currents for the second discharge were measured, shown in Fig. 10c, and are observed to be directly proportional to the second discharge voltage in a linear fashion, with the angular coefficient proportional to the main discharge voltage. It can be seen that even when the second discharge capacitor has 0 V there is a considerable current flowing. This minimum current is proportional to the main discharge voltage.

The first regimen of the secondary discharge is largely dependent on the main discharge that, in fact, generates current between the secondary electrodes even when its capacitor is completely discharged.

The second regimen shows an oscillatory discharge with an offset, given by the increased voltage in the secondary discharge. A critically dumped discharge is observed after the end of the main discharge, although not very pronounced. The third regimen shows a more pronounced critically dumped phase after the main discharge ended and the fourth regimen shows an even more pronounced critically dumped behaviour.

After the main discharge is over, there is no more plasma being produced upstream and the propellant starts to produce the LTA. As a first hypothesis, the current flowing in the secondary electrodes, at this point, would supposedly be flowing in the LTA. A more in-depth analysis will be carried out to validate this hypothesis.

Tests measuring the length of the discharge showed an increasing length of discharge with the second discharge voltage, but also indicated that, for a given main discharge voltage, there is a maximum length of the secondary discharge. This characteristic supports the hypothesis that the secondary current discharge would be flowing on the LTA, as there is a limited amount of LTA for a given main discharge voltage. In fact, a residual voltage was measured in the secondary capacitor for secondary discharge voltages above 200 V.

The maximum delays observed at different secondary discharge voltages indicate that the transition of the secondary discharge from an oscillatory mode, with the first part negative, to a completely positive discharge occurs at different voltages, depending on the main discharge voltage. As it can be observed when there is 0 V applied on the secondary capacitor, a current on the secondary electrodes is generated by the main discharge with the first bit negative. To overcome this first negative bit and initiate the positive only discharge current it is necessary to have increasingly more voltage on the secondary capacitor as the main discharge voltage is increased. These voltages can be seen as the voltages above which the discharge is completely positive. A finer change in the secondary discharge voltages is required to analyze exactly where the peak occurs and the behavior in its vicinity.

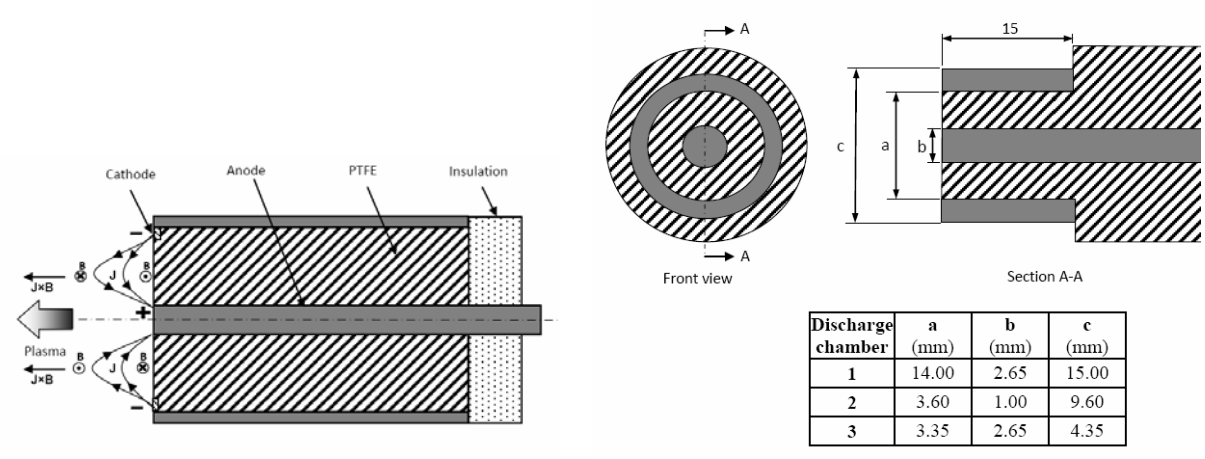

Discharge chamber	a (mm)	b (mm)	c (mm)
1	14.00	2.65	15.00
2	3.60	1.00	9.60
3	3.35	2.65	4.35

a) b)

Figure 6. PPT in a coaxial geometry (a) and schematic diagram of the discharge chambers tested (b).

Table 2. Test parameters and results from the first three coaxial prototypes tested in 2003.

	Discharge Chamber		**1**	**2**	**3**
Parameters	Chamber mass before test (g)		67.3355	5.99092	3.94783
	Chamber mass after test (g)		67.3342	5.98649	3.93797
	Internal electrode diameter (mm)		2.65	1	2.65
	Propellant diameter (mm)		14	3.6	3.35
	Operation time	Hours (h)	92	29	09
		Minutes (min)	48	07	10
Calculated values	Exposed propellant area (mm2)		148.42	9.39	3.30
	Pulse energy / Propellant area (J/mm2)		0.0844	1.3332	3.7964
	Test time (s)		334080	104820	33000
	Total number of pulses		334080	104820	33000
	Total mass consumption (g)		1.30E–03	4.43E–03	9.86E–03
	Mass consumption per pulse (g)		3.89E–09	4.23E–08	2.99E–07
	Pulse energy (J)		12.52	12.52	12.52
	Total energy input (J)		4.18E+06	1.31E+06	4.13E+05
	Vaporized mass per Joule (g/J)		3.11E–10	3.37E–09	2.39E–08
	Total mass consumption (mg)		1.3	4.43	9.86
	Mass consumption per pulse (µg)		0.00389	0.0423	0.299
	Consumed mass / energy (µg/J)		0.00031	0.00337	0.0238

Figure 7. The three prototypes shown before, during and after the tests.

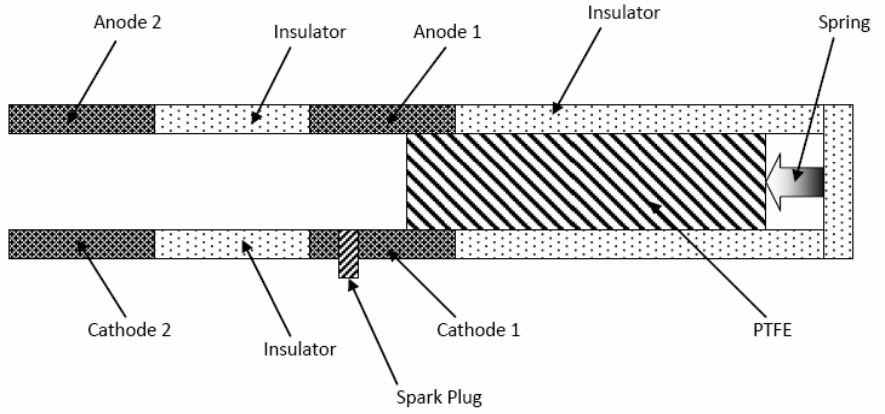

Figure 8. HFB-PPT discharge chamber.

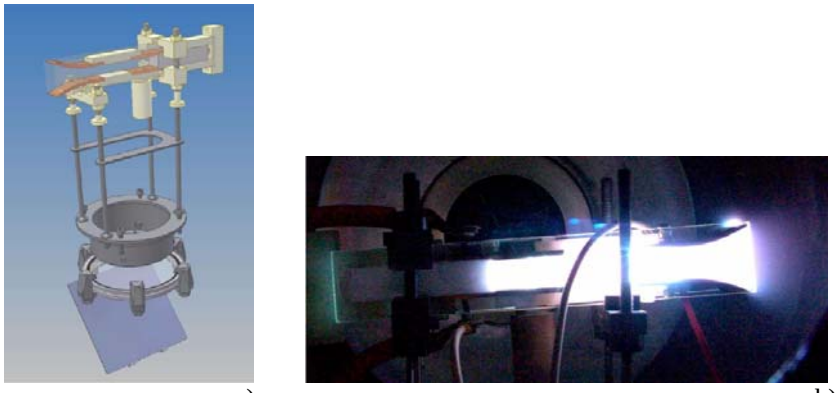

a) b)

Figure 9. The model of developed HFB-PPT (top) mounted on its support (centre) with a mirror on the botton for instrumentation purposes (a) and HFB-PPT firing (b).

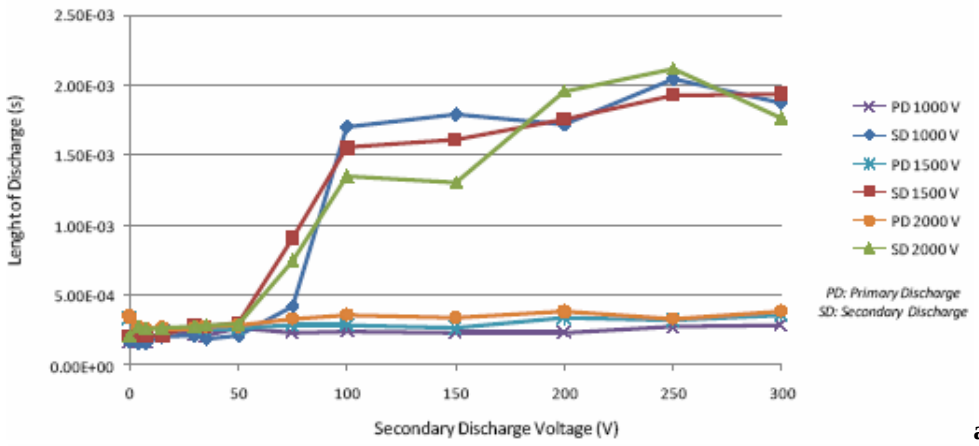

a)

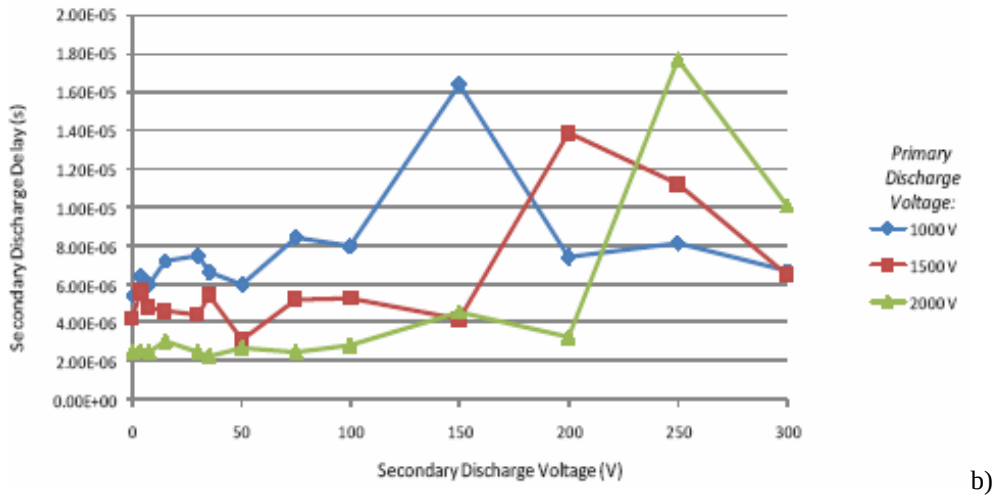

b)

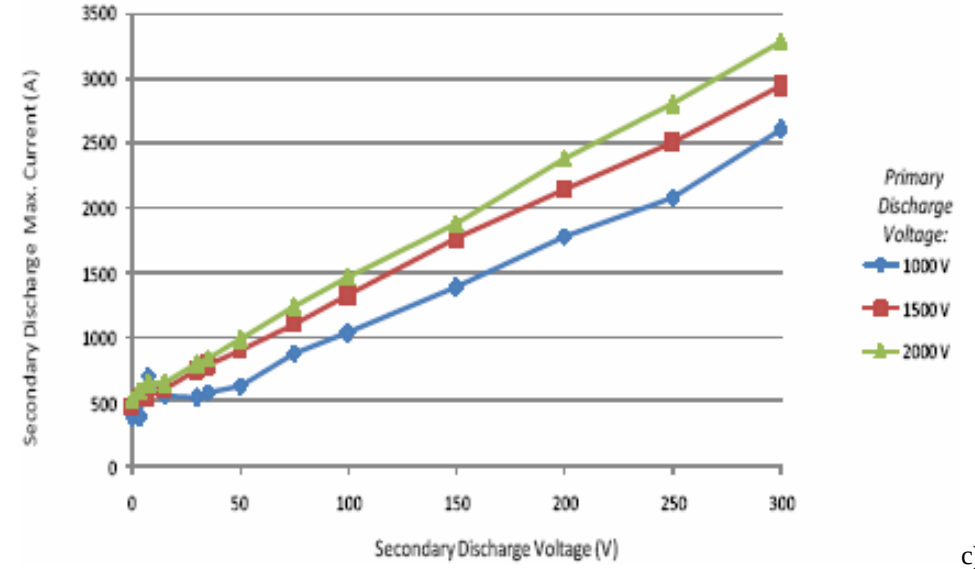

c)

Figure 10. Length of the secondary discharge (a), delay between the first discharge and the second discharge (b) and maximum current in the secondary discharge all as function of the voltage applied in the secondary electrodes for three different primary discharge voltages.

B. Electric Propulsion at University of Brasilia (UnB)

5. *Past and present Hall thrusters*

José L. Ferreira and students started the ground-based performance tests with its first Hall thruster prototype in 2003 at the Plasma Laboratory at the University of Brasilia (UnB). The first Hall thruster prototype consisted of a 28-cm diameter by 4-cm long stainless steel discharge chamber with a 3.5-cm large ionization channel insulated by a thin ceramic cement layer within 2mm thickness. The anode consisted of a stainless steel ring seizing 2cm wide and 1mm thick, located 3.8-cm from the exit of the channel. Behind the anode ring the propellant gas could be uniformly distributed in the Hall plasma source chamber by using an insulated cupper circular tube with several small holes. The magnetic field was generated by a ring composed of several ferrite permanent magnets surrounding the discharge chamber. A movable tungsten filament painted with a layer of carbonates (Ba, Ca, Sr)CO_3 was used as primary electron emitter. The plasma diagnostics inside and outside the source were carried out by using both a movable Langmuir probe and an ion energy analyzer. This Hall thruster, shown schematically in Fig. 6a and assembled on the work bench in Fig. 6b, could produce an estimated thrust of 85 mN and an estimated specific impulse of 1083 s in high discharge current mode, and 26 mN and 901s in low discharge current mode, both modes using argon as propellant. Table 3 summarizes the performance characteristics of the first Hall thruster prototype. The extracted plasmas for high and low current modes are shown in Fig 6c and 6d, respectively.

The second prototype of Hall thruster is presently under construction and adopts the same concept of its predecessor, except by the following: a smaller discharge chamber with diameter of 15.5 cm, the replacement of the internal insulator by a sintered alumina case, the replacement of ferrite permanent magnets by NdFe permanent magnets, and the use of hollow cathodes instead of tungsten filaments for plasma generation. The plasma diagnostics will involve, besides the instrumentation mentioned above, a Doppler line broadening equipment developed as a non-invasive technique for the ion temperature measurement. The development of this Hall Thruster is under contract with the UNIESPAÇO program at the Brazilian Space Agency.

Table 3. Performance parameters and results from the first Hall thruster prototypes tested in 2003.

	High current	Low current
Maximum thrust available (mN)	126	126
Maximum thrust density (N/m2)	6.94	6.94
Measured thrust (mN)	84.9	26.5
Measured thrust density (N/m2)	4.68	1.46
Maximum specific impulse (s)	1607	1607
Average specific impulse (s)	1083	901
Ionized mass rate (%)	3.30	5.76
Electrical efficiency (%)	33.9	67.2
Total efficiency (%)	1.12	3.87

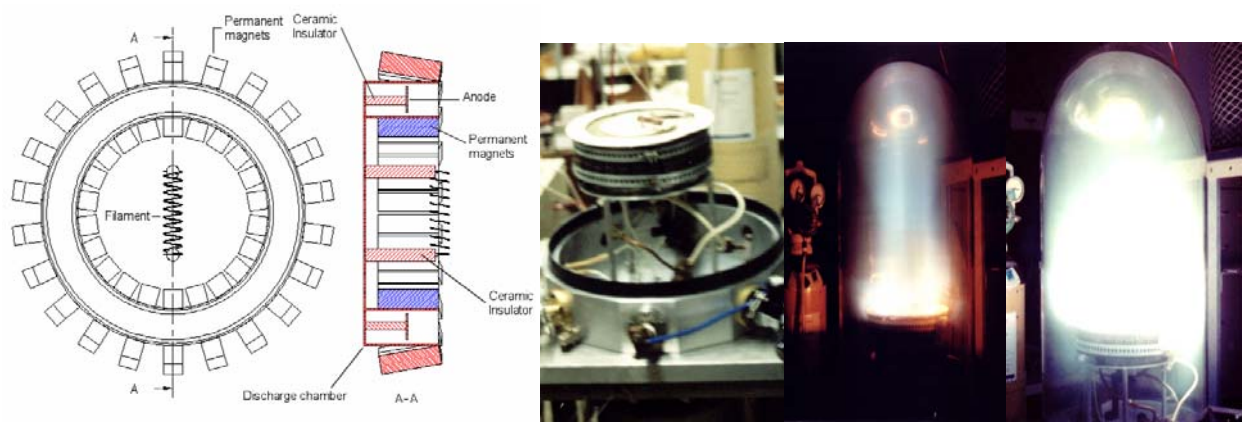

a) b) c) d)

Figure 6. The first prototype of Hall thruster at UnB: schematics (a), assembled on the work bench (b), and firing in both low and high current modes (c) and (d), respectively

Appendix

Thrust: $$T = I_B \sqrt{\frac{2mU}{q}} \quad (1)$$

In this paper the thrust has been estimated assuming singly-charged ion beams.

Specific impulse: $$I_s = \frac{T}{\dot{m} g_o} \quad (2)$$

Acknowledgments

The authors thank to Fernando de Souza Costa at the INPE-LCP and José Leonardo Ferreira at University of Brasilia for the contributing texts on the development of PPTs and Hall thrusters.

References

[1]Sandonato, G. M., and Barroso, J. J., "Conceptual Design of a Beam Extraction Electrode System for a 1 mN Ion Thruster," *Rev. Sci. Instruments*, Vol. 67, No. 4, 1996, pp. 1486, 1492.

[2]Sandonato, G. M., Barroso, J. J., and Montes, A., "Magnetic Confinement Studies for Performance Enhancement of a 5-cm Ion Thruster," *IEEE Trans. on Plasma Science*, Vol. 24, No. 6, 1996, pp. 1319, 1329.

[3]Sandonato, G. M., Lima, P. E., and Otani, C., "The Influence of the Magnetic Field Strength on the Magnetic Confinement of Primary Electrons in an Ion Source," *Contrib. Plasma Physics*, Vol. 39, No. 3, 1999, pp., 187, 195.

[4]Burton, R. L. and Turchi, P. J., "Pulsed Plasma Thruster," *Journal of Propulsion and Power*, Vol. 14, No. 5, 1998, pp. 716, 735.

[5]Choueiri, E. Y., "System Optimization of Ablative Pulsed Plasma Thruster for Station keeping," *Journal of Spacecraft and Rockets*, Vol. 33, No. 1, 1996, pp. 96, 100.

[6]Yang, T. F., Liu, P., Chang-Diaz, F. R., Lander, H., Childs, R. A., Becker, H. D. and Fairfax, S. A., "A Double Pendulum Plasma Thrust Balance and Thrust Measurement at a Tandem Mirror Exhaust," *Review of Scientific Instruments*, Vol. 66, 1995, pp. 4637-4643.

[7]Paccani, G. and Ravignani, R., "Sulla Misura Indiretta della Spinta di Propulsori Elettrici," *Aerotecnica Missili e Spazio*, Vol. 74, 1995, pp. 103-110.

[8]Chavers, D. G., Chang-Diaz, F. R., Irvine, C. and Squire, J. P., "Momentum and Heat Flux Measurements in the Exhaust of VASIMR Using Helium Propellant," IEPC-03-028, *28th International Electric Propulsion Conference*, Toulouse, France, 2003.

[9]Kimura, I., Yanagi, R. and Inoue, S., "Preliminary Experiments on Pulsed Plasma Thrusters with Applied Magnetic Fields," AIAA-78-655, *AIAA/DGLR 13th International Electric Propulsion Conference*, San Diego, CA, 1978, 6 p.

[10]Yanagi, R. and Kimura, I., "A New Type Target for the Measurement of Impulse Bits of Pulsed Plasma Thrusters", *Journal of Spacecraft and Rockets*, Vol. 39, No. 3, 1982, pp. 246, 249

[11]Kameoka, M., Takegahara, H., Shimizu, Y. and Toki, K., "Single Impulse Measurement of a Coaxial Pulsed Plasma Thruster," IEPC-03-093, *28th International Electric Propulsion Conference*, Toulouse, France, 2003.

[12]Marques, R. I. *Desenvolvimento de um Propulsor de Plasma Pulsado.* M.Sc. Thesis (in Portuguese), São José dos Campos, INPE - Instituto Nacional de Pesquisas Espaciais, 2004.

[13]Pottinger, S. J., P. Gessini, D. Webb, R. Intini Marques, and S.B. Gabriel. "Electric Propulsion Research at the University of Southampton." *Journal of the British Interplanetary Society (JBIS)*, Vol. 59, No. 5, 2006, pp. 176, 185.